Spatial Vector Solitons in Nonlinear Photonic Crystal Fibers

By José R. Salgueiro, Yuri S. Kivshar, Dmitry E. Pelinovsky,
Verónica Simón, and Humberto Michinel

We study *spatial vector solitons* in a photonic crystal fiber (PCF) made of a material with the focusing Kerr nonlinearity. We show that such two-component localized nonlinear waves consist of two mutually trapped components confined by the PCF linear and the self-induced nonlinear refractive indices, and they bifurcate from the corresponding scalar solitons. We demonstrate that, in a sharp contrast with an entirely homogeneous nonlinear Kerr medium where both scalar and vector spatial solitons are unstable and may collapse, the periodic structure of PCF can stabilize the otherwise unstable two-dimensional spatial optical solitons. We apply the matrix criterion for stability of these two-parameter solitons, and verify it by direct numerical simulations.

1. Introduction

Photonic crystal fibers (PCF) have attracted much interest due to their intriguing properties, many potential applications, as well as the recent development of successful technologies for their fabrication with engineered linear and nonlinear properties [1, 2]. Photonic crystal fibers are characterized by a conventional cylindric geometry with a two-dimensional lattice of air holes running parallel

to the fiber optical axis. Such PCF structures share the propagation properties of *photonic crystals*, based on the existence of the frequency gap with the transmission suppressed due to the Bragg scattering, as well as the properties of conventional *optical fibers*, due to the presence of a defect in the structure acting as a PCF core. Some of the PCF intriguing characteristics include the possibility to design single-moded PCFs independently on the light frequency even for a large core, allowing the guidance of high powers what makes PCFs very suitable for amplifiers or laser cavity applications. On the other hand, there exists an upper cut-off frequency by means of a reduction of the core index, and this also allows a very flexible control on the dispersion properties, supporting large shifts of the zero-dispersion point, and birefringence, which can be made much higher than in conventional fibers by a proper design.

In PCFs, light confinement is restricted to the core of the fiber and therefore nonlinear effects, such as light self-trapping and localization in the form of spatial optical solitons [3], may become important. The stabilizing effect of periodic media for optical solitons has been observed in a number of cases. In particular, one-dimensional vector solitons that are unstable in uniform media are stable in a medium with a periodic modulation of the refractive index [4]. Also, discrete vector solitons were experimentally observed in two-dimensional optically induced photonic lattices [5]. Similar to the case of two-dimensional nonlinear photonic crystals [6], it has been recently demonstrated numerically that a PCF can support and stabilize both fundamental and vortex spatial optical solitons [7, 8]. In sharp contrast with an entirely homogeneous nonlinear Kerr medium where spatial solitons are unstable and may collapse, it was shown that the periodic structure of PCF can stabilize the otherwise unstable two-dimensional spatial optical solitons.

In this paper, we make a further step forward in the study of nonlinear effects in PCFs, in comparison with the recent analysis [7, 8], and analyze the existence and stability of spatial vector solitons in PCFs. In general, vector solitons are defined as two-component mutually trapped localized beams whose properties may differ substantially from the properties of one-component scalar solitons [3]. In addition, two-dimensional vector solitons are known to be unstable in the nonlinear Kerr medium [9]. In contrast, as we show in this paper, the periodic modulation of the refractive index in the PCF provides an effective physical mechanism to stabilize the otherwise unstable two-dimensional spatial optical solitons. We study the stability of these two-parameter solitons and apply the matrix stability criterion that is then verified by direct numerical simulations.

The structure of this paper is as follows. First, in Section 2 we introduce our physical model that is characterized by an effective potential created by the PCF environment and also describe the nonlinear interaction between the beam components. Then, in Section 3 we introduce our numerical method to find the classes of spatially localized modes existing in the nonlinear core of the PCF. In Section 4 we describe the family of two-component spatial solitons. Finally, in Section 5 the stability of both one- and two-component solitons is analyzed.
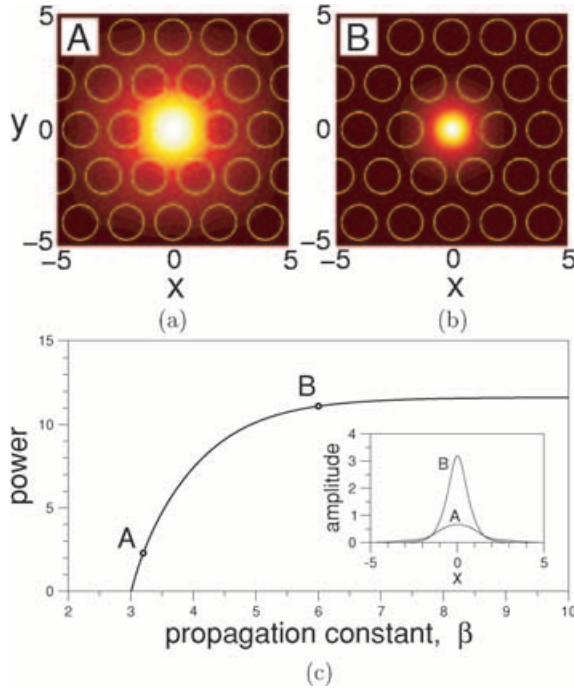
Figure 1.   (a,b) Examples of stationary solutions for scalar PCF spatial solitons for $\beta = 3.2$ and $\beta = 6$, and (c) power dependence of the soliton family. Points A and B in the power diagram (c) correspond to the examples (a,b), respectively. Inset: the corresponding one-dimensional profiles at $y = 0$ for both examples.

2. Model

We consider a simple model of PCF that describes, at a given frequency, the spatial distribution of light in a nonlinear dielectric material with a triangular lattice of air holes in a circular geometry. We assume that the PCF material possesses a nonlinear Kerr response, and the hole at the center is filled by the same material creating a nonlinear defect, as shown in Figures 1(a) and (b). In the substrate material of the fiber, the linear refractive index is n_s, whereas inside the holes it is n_a. Air holes have radius r. We consider the case when the PCF core guides two modes or two orthogonal polarizations. In the nonlinear regime, the mutual interaction between these two modes is described by the system of coupled equations,

$$i\frac{\partial \psi_1}{\partial z} + \Delta \psi_1 + n_a \psi_1 + V(x, y)\left(\delta + |\psi_1|^2 + \mu |\psi_2|^2\right)\psi_1 = 0,$$
$$i\frac{\partial \psi_2}{\partial z} + \Delta \psi_2 + n_a \psi_2 + V(x, y)\left(\delta + |\psi_2|^2 + \mu |\psi_1|^2\right)\psi_2 = 0,$$

$$(1)$$

where ψ_1 and ψ_2 are two components (or two polarizations) of the electric field, Δ is a transversal Laplace operator in (x, y), $\delta = n_s - n_a$, and $V(x, y)$ is an effective potential describing the defect and the lattice of holes in the transverse plane (x, y). We normalize $V = 1$ in the material outside the holes, and $V = 0$ in the holes. The nonlinear incoherent interaction between the components is described by the parameter μ.

To find stationary two-dimensional nonlinear modes of PCF, we look for the solutions in the form

$$\psi_1(x, y, z) = u(x, y)e^{i\beta z}, \quad \psi_2(x, y, z) = v(x, y)e^{i\gamma z},$$

and obtain the following coupled system of z-independent differential equations:

$$
\begin{aligned}
\beta u &= \Delta u + n_a u + V(x, y)(\delta + u^2 + \mu v^2)u, \\
\gamma v &= \Delta v + n_a v + V(x, y)(\delta + v^2 + \mu u^2)v.
\end{aligned}
\tag{2}
$$

The model (2) describes the stationary distribution of a two-component field in an inhomogeneous nonlinear medium, in a planar geometry. Without the external potential, the vector solitons in both one- and two-dimensional cases have been studied earlier [3]. However, the lattice of air holes and the central defect break the radial symmetry of the problem, and the corresponding vector solitons are not radially symmetric.

3. Numerical method

To find the solutions for nonlinear localized modes, we consider a rectangular domain of the (x,y) and apply a finite-difference scheme, taking n and m uniformly distributed samples of the variables x and y, respectively, to cover all the domain. Denoting those samples as x_i, $1 \le i \le n$, and y_j, $1 \le j \le m$, at each mapped point (x_i, y_j) of the domain we consider the corresponding samples for all the functions defined in the equations: $u_{ij} = u(x_i, y_j)$ and, similarly, the second component v_{ij}, and the potential V_{ij}. Substituting these redefined variables into the model (2), and imposing homogeneous boundary conditions in all four edges of the domain, we obtain an algebraic nonlinear problem of $2 \times n \times m$ equations with the same number of unknowns u_{ij} and v_{ij}.

To make the notation more compact, the samples corresponding to different functions, which constitute $n \times m$ matrices, are rearranged concatenating the columns of the matrices to produce big column vectors of N rows ($N = n \times m$), $\mathbf{u}$, $\mathbf{v}$, and $\mathbf{V}$. Besides, we compact the vectors corresponding to both field components in a unique field vector, by concatenating one after another, $\mathbf{q} = (\mathbf{u}^T \,|\, \mathbf{v}^T)^T$, with $2N$ components q_k. In that way, the algebraic nonlinear system can be written as $\mathbf{Aq} = 0$, where $\mathbf{A}$ is the $2N \times 2N$ matrix, which

depends on the unknown vector through the nonlinear terms, and we denote it as $\mathbf{A[q]}$. The system of equations takes the form

$$\mathbf{A[q]q} = 0, \tag{3}$$

being the rows of the matrix product

$$E_k = \Sigma_j (\mathbf{A[q]})_{kj} q_j, \tag{4}$$

so that the system is written as $E_k = 0$, $k = 1, 2, \ldots, 2N$. The matrix $\mathbf{A}$, even being huge in size, is in practice very sparse, and it differs from zero at the main diagonal, two diagonals next to the main one, and two more at the distance n from the main one (these four diagonals appear due to the coupling terms in the derivatives of the Laplace operator), and also two more diagonals at a distance N from the main one, due to the coupling between both field components.

The nonlinear system of Equation (3) can be solved using the standard globally convergent Newton method [10, 11], which builds the solution iteratively from an initial guess $\mathbf{q}^0$ in the form $\mathbf{q}^l = \mathbf{q}^{l-1} + \delta \mathbf{q}$, $l = 1, 2, \ldots$, where the calculation of the so-called Newton step $\delta \mathbf{q}$ at each iteration involves the solution of the linear system

$$\mathbf{J}(\delta \mathbf{q}) = -\mathbf{E}, \tag{5}$$

where $\mathbf{E}$ is the vector obtained by substituting the last iterate into Equation (4), and $\mathbf{J}$ is the Jacobian matrix defined as $J_{ij} = \partial E_i / \partial q_j$, and also evaluated substituting the last known iterate. The Jacobian matrix presents a similar sparse structure as the matrix $\mathbf{A}$, and it can be calculated analytically. Obviously, due to a huge size of the matrix $\mathbf{J}$, the system (5) can only be solved iteratively. Taking into account that for our particular problem the matrix $\mathbf{J}$ is symmetric, though in general indefinite, the SYMMLQ method [12] proved to be successful.

Some improvements are possible in the method, taking the advantage of the system symmetries. In fact, due to the hexagonal lattice of holes, the field should be invariant under the rotation by the angles $l(\pi/3)$, where l is an integer. It would make possible to solve the problem only in a circular sector of the amplitude $\pi/3$, imposing periodic boundary conditions at the borders and homogeneous in the radial direction. The number of points could be reduced in that case by the factor of six. Another approach, that took advantage of the lattice periodicity, was developed by Ferrando et al. [7].

4. Stationary solutions

The presence of the external linear potential given by the central defect and the lattice of air-holes makes the system nonscalable and its radial symmetry broken. Therefore, the study has to be carried out by numerical methods. We

solve Equation (2) numerically for both scalar (when one of the components vanishes, i.e., $v = 0$) and vector (or two-component) spatial solitons and obtain the stationary states of the nonlinear system.

4.1. Scalar solitons

For the scalar case, we assume that one of the components is absent (e.g., $v = 0$) and we study a single nonlinear equation of the nonlinear eigenvalue problem (2). We find a family of the spatially localized modes—the so-called PCF spatial solitons—as a function of the mode propagation number β. These results are similar to those earlier reported by Ferrando et al. [7], and the solution can be envisaged as the fundamental mode of the effective fiber generated by the combined effect of the PCF refractive index and the nonlinear index induced by the solution amplitude itself.

Figures 1(a) and (b) show two examples of stationary, spatially localized solutions of the nonlinear model (2) at $v = 0$, which describe scalar spatial optical solitons as nonlinear modes of PCF. The whole family of such one-parameter solutions can be characterized by the power $P = \int u^2 dx dy$, that is plotted in Figure 1(c), where the points A and B correspond to the examples (a,b), respectively. The material parameters for the PCF are taken as $n_a = 1$, $n_s = 4$, and $r = 0.75$.

First, we note that these stationary solutions for scalar spatial solitons in PCF have been found earlier by Ferrando et al. [7], who also mentioned, without a proof, that such nonlinear modes are stabilized by the lattices of PCF holes. Indeed, it is well known that in the nonlinear focusing Kerr media without a nonlinearity saturation, the self-trapped optical beams are always unstable [3]. This instability can manifest itself as the beam spreading, when the input power is lower than that of the soliton, or the beam collapse, when the power is larger than the soliton power. As has been mentioned earlier by Ferrando et al. [7], such a soliton instability can be suppressed by the presence of the lattice of holes, because the external potential stops the beam spreading, as it happens in a conventional optical fiber, leading to the existence of a family of stable stationary beams.

To demonstrate this feature, we follow the standard analysis of the soliton stability [3] and plot in Figure 1(c) the soliton power as a function of the soliton propagation constant. A positive slope of this dependence indicates the soliton stability, as will be demonstrated below. In Figure 2 we present some related numerical simulations of the dynamics of a perturbed scalar soliton. Some of the stationary states are scaled by factors slightly higher and lower than unity, respectively, so as to induce an initial perturbation, and then propagated using a standard beam-propagation-method algorithm. The result is that the soliton behaves stably if its power remains below the maximal limiting power on Figure 1(c).
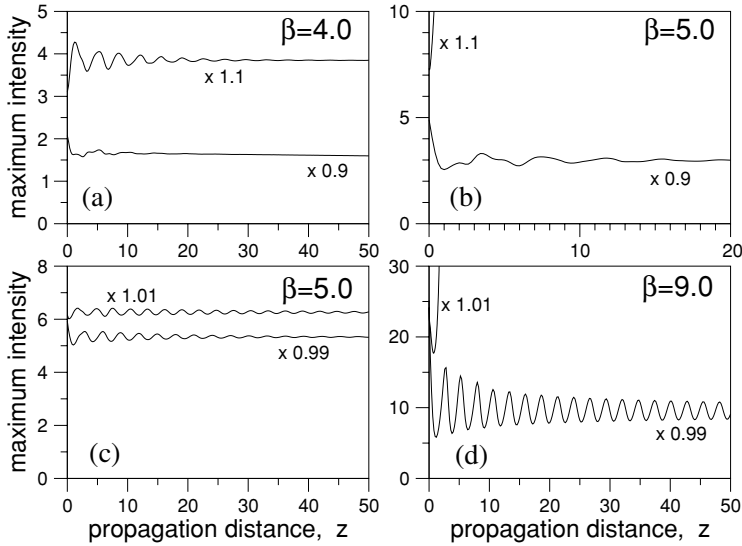
Figure 2. Results of numerical simulations of the soliton dynamics in the scalar case. The initial stationary solution is perturbed by two amplitude scalings (indicated in the graphs): one is higher and the other one is lower than the unity. Shown is the maximum soliton intensity versus the propagation distance.

When the scaling factor is taken higher than unity, a stable propagation is observed for the solitons of low enough power, as seen in Figure 2(a). Nevertheless, for higher values of the power the soliton may collapse if the scaling factor is too large (Figure 2(b)), but it remains stable for a smaller scaling (Figure 2(c)). Further increase in the initial power results in collapse of the beam for any scaling factor (Figure 2(d)).

When the scaling factor is taken smaller than unity, the lattice of holes stops the soliton spreading in all cases, so that the soliton propagates stable, as is illustrated in all cases presented in Figure 2.

4.2. Vector solitons

Vector solitons in the coupled problem (2) depend on both propagation constants (β, γ) as well as the material parameters (δ, μ). Some examples of the vector solitons in PCF are presented in Figure 3, corresponding to the points A and B marked on the existence domain shown in Figure 4. This domain, whose symmetry respect to both parameters β and γ is evident from the symmetry of both the equations of the model (2), is plotted in the plane (β, γ). The existence domain is limited by two lines at whose points (bifurcation points) the vector solitons originate from the scalar solitons; such curves can be regarded as *bifurcation curves*. When $\mu < 1$, close to the
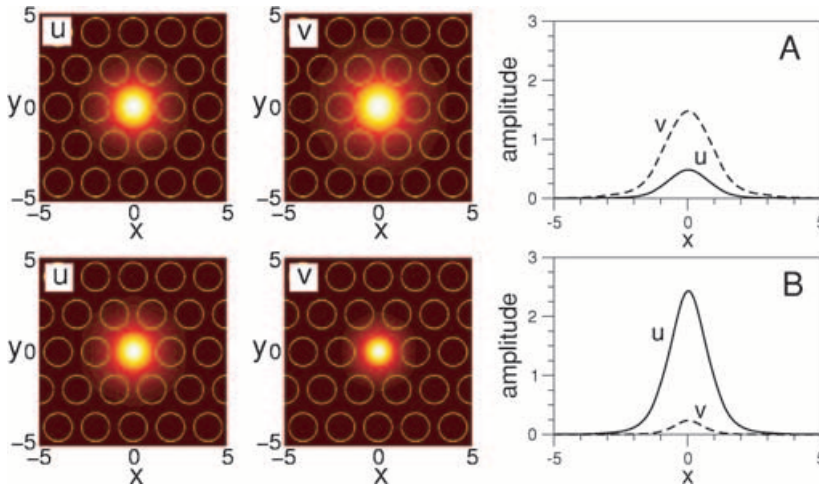
Figure 3. Examples of the two-component stationary solutions of the model (2) for vector solitons in PCFs. Two cases correspond to the points A ($\beta = 5$, $\gamma = 4$) and B ($\beta = 5$, $\gamma = 8$) in the existence domain shown in Figure 4 for $\mu = 2$. In each column both components are shown in the plane (x, y), together with a one-dimensional x-cutoff profile to compare the field amplitudes.

lower bifurcation curve, the second component decreases becoming a linear guided mode of the soliton mode in the first (self-guided) component; the opposite case occurs close to the upper bifurcation curve where the role of the components is reversed. When $\mu > 1$, we have the opposed situation with
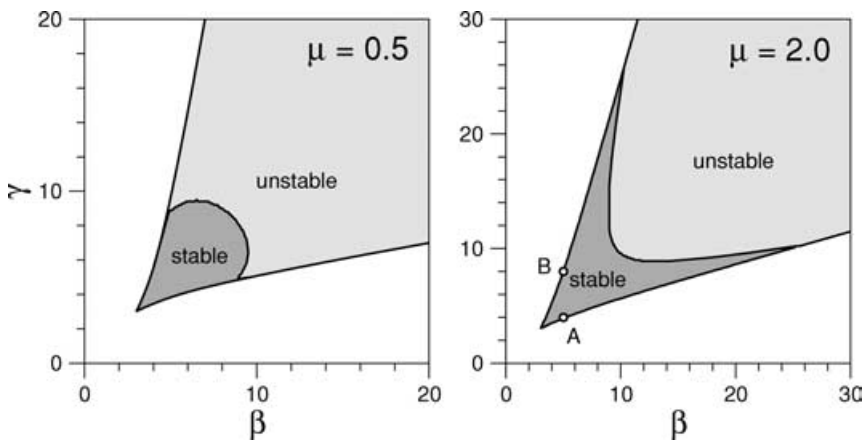

Figure 4. Existence domain for the vector solitons in PCF in the plane (β, γ), shown at two values of the coupling parameter μ. Labeled points correspond to two particular examples shown in Figure 3.

respect to the lower and upper bifurcation curves. The presence of an effective waveguide associated with one missing hole in the lattice is the reason that the propagation constants take a value different from zero, when the power vanishes; this threshold value corresponds to the eigenvalue of the linear mode guided by this effective waveguide in the lattice of air holes.

Similar to the scalar case, the presence of a periodic lattice of holes suggests that the vector solitons may become stable in this system. In this case, the vectorial nature of the system plays an important role to determine the portion of the domain where the solutions are stable. As follows from the next section, by applying the generalized matrix stability criterion, it is possible to determine the boundary between the stable and unstable regions. According to that, this boundary is the set of points that fulfill the marginal stability condition $\det(D) = 0$, where $D_{ij} = \partial P_i / \partial \beta_j$ while (P_1, P_2) and (β_1, β_2) are, respectively, powers and propagation constants for the components (u, v). In Figure 4 this boundary, as well as both regions of stability and instability are represented. A number of numerical simulations were carried out to test the stability of the solutions in each region. A standard beam propagation algorithm was used and the stationary solutions of the system were rescaled by a constant slightly higher that one, so that the peak amplitude of the fields initially raises over the peak amplitude of the exact stationary solution. For fields in the stability region, in spite of the initial growth of amplitude, it becomes stable after certain propagation distance.

5. Soliton stability

Stability of scalar and vector solitons in the coupled NLS equation can be studied with the matrix stability criterion [13, 14]. Applications of the matrix criterion depend on the exact count on the number of eigenvalues of the matrix Schrödinger operators and require careful numerical computations of a spectral (linearization) problem. Alternatively, a count of the eigenvalues can be developed in a local neighborhood of the bifurcation curves, such as the ones shown on Figure 4. These computations can be developed analytically, with the perturbation series expansions [15–17].

5.1. Scalar solitons

For simplicity and without loss of generality, we set $n_a = 0$ in our analytical computations. First, we study the stability of scalar solitons, when $u = \phi(x, y)$ and $v = 0$, where $\phi(x, y)$ is a solution of the nonlinear eigenvalue problem

$$\Delta\phi - \beta\phi + V(x, y)(\delta + \phi^2)\phi = 0, \tag{6}$$

We assume that there exists a ground-state (positive definite) solution of the linear problem

$$\Delta\phi_0 - \beta_0\phi_0 + \delta V(x, y)\phi_0 = 0,$$

with the propagation constant β_0. Applying the local bifurcation analysis for the nonlinear ground state, we look for the solutions in the asymptotic form, $\phi = \epsilon[\phi_0 + \epsilon^2\phi_2 + O(\epsilon^4)]$ and $\beta = \beta_0 + \epsilon^2\beta_2 + O(\epsilon^4)$, and obtain the result

$$\beta_2 = \frac{(\phi_0^2, V(x, y)\phi_0^2)}{(\phi_0, \phi_0)} > 0, \tag{7}$$

where the inequality follows from the fact that $V(x, y)$ is nonnegative. Therefore, the soliton power (squared L^2 norm) $p(\beta) = \|\phi\|_{L^2}^2 = (\phi, \phi)$ is an increasing function of the propagation constant β near the bifurcation point $\beta = \beta_0$:

$$\frac{dp}{d\beta} = \frac{(\phi_0, \phi_0)}{\beta_2} + O(\epsilon^2) > 0. \tag{8}$$

Stability for the scalar solitons is determined by the linear eigenvalue problem, $L_+u = -\lambda w$ and $L_-w = \lambda u$, where the linear operators $L_\pm$ are defined as

$$L_+ = \beta - \Delta - V(x, y)(\delta + 3\phi^2(x, y)),$$
$$L_- = \beta - \Delta - V(x, y)(\delta + \phi^2(x, y)).$$

If $\phi(x, y) > 0$ for all $(x, y) \in R^2$, then L_- is nonnegative with the zero eigenvalue $L_-\phi = 0$ due to the gauge invariance. We consider the number of negative eigenvalues of L_+ and apply the earlier results for one-dimensional solitons [13]. It is clear that L_+ must have at least one negative eigenvalue because

$$(\phi, L_+\phi) = -2(\phi^2, V(x, y)\phi^2) < 0. \tag{9}$$

When $\beta = \beta_0$ and $\phi = 0$, the operator L_+ has a simple zero eigenvalue and no negative eigenvalues. Therefore, according to the perturbation theory, the operator L_+ has exactly *one negative eigenvalue* for $\beta > \beta_0$ near the local bifurcation threshold. The condition for applicability of the Vakhitov–Kolokolov criterion is satisfied and it suggests stability of scalar solitons at least near the bifurcation point.

Numerically, we have checked that the number of negative eigenvalues of L_+ does not change and the slope of $dP/d\beta$ is always positive, as shown in the example presented in Figure 1(c). Therefore, the scalar optical solitons in PCF is stable everywhere for $\beta > \beta_0$.

5.2. Vector solitons

Next, we study stability of vector solitons, when $u = \Phi(x, y)$ and $v = \Psi(x, y)$, where $\Phi(x, y)$ and $\Psi(x, y)$ are real-valued positive solutions of the coupled

nonlinear eigenvalue problem

$$\beta\Phi = \Delta\Phi + V(x, y)(\delta + \Phi^2 + \mu\Psi^2)\Phi,$$
$$\gamma\Psi = \Delta\Psi + V(x, y)(\delta + \mu\Phi^2 + \Psi^2)\Psi. \tag{10}$$

We consider a local bifurcation of the vector soliton from the scalar one, and look for solutions in the asymptotic form, $\Phi = \Phi_0 + \epsilon^2\Phi_2 + O(\epsilon^4)$ and $\Psi = \epsilon(\Psi_0 + \epsilon^2\Psi_2 + O(\epsilon^4))$, and also expand the eigenvalue, $\gamma = \gamma_0 + \epsilon^2\gamma_2 + O(\epsilon^4)$, where β is an arbitrary parameter, such that $\beta > \beta_0$. The function $\Phi_0 = \phi(x, y)$ satisfies the nonlinear eigenvalue problem (6) for a scalar soliton. Function $\Psi_0 = \psi(x, y)$ is a ground-state solution of the linear eigenvalue problem

$$L_0\psi = (\gamma_0 - \Delta - V(x, y)(\delta + \mu\phi^2))\psi = 0, \tag{11}$$

where γ_0 is a function of parameters (δ, μ) and the propagation constant β. The problem for $\Phi_2(x, y)$, $L_+\Phi_2 = \mu V(x, y)\phi\psi^2$, is always solvable, in the assumption that the operator L_+ for the scalar soliton has one negative and no zero eigenvalues for any $\beta > \beta_0$. Finally, from the solvability condition of the linear inhomogeneous problem

$$L_0\Psi_2 = 2\mu V(x, y)\phi\psi\Phi_2 + V(x, y)\psi^3 - \gamma_2\psi, \tag{12}$$

we derive that

$$\gamma_2 = \frac{2\mu(\psi^2, V(x, y)\phi\Phi_2) + (\psi^2, V(x, y)\psi^2)}{(\psi, \psi)}.$$

Numerical results show that $\gamma_2 > 0$ for $\mu < 1$ (i.e., the bifurcation occurs from the lower boundary of the existence domain on the plane (β, γ)), $\gamma_2 < 0$ for $\mu > 1$ (i.e., bifurcation occurs from the upper boundary of the existence domain), and $\gamma_2 = 0$ for $\mu = 1$ (i.e., the existence domain shrinks on the diagonal $\gamma = \beta > \beta_0$ and $\gamma_0 = \beta_0$).

We compute the Hessian matrix of derivatives of individual powers $P = (\Phi, \Phi)$ and $Q = (\Psi, \Psi)$ with respect to parameters β and γ. Let $p = (\phi, \phi)$ and assume that $p'(\beta) > 0$ for scalar soliton with $\beta > \beta_0$. Near the local bifurcation threshold at $\gamma = \gamma_0$, we have

$$\frac{\partial P}{\partial\gamma} = \frac{2(\phi, \Phi_2)}{\gamma_2} + O(\epsilon^2) = \frac{\partial Q}{\partial\beta}, \quad \frac{\partial Q}{\partial\gamma} = \frac{(\psi, \psi)}{\gamma_2} + O(\epsilon^2), \tag{13}$$

such that the determinant of the Hessian matrix is

$$D(\beta, \gamma) = \frac{(\psi, \psi)p'(\beta)}{\gamma_2} - \frac{4(\phi, \Phi_2)^2}{\gamma_2^2} + O(\epsilon^2). \tag{14}$$

When $\mu < 1$, we have $\gamma_2 > 0$ and the determinant may change the sign. Numerical results show that $D > 0$ for $\beta_0 < \beta < \beta_*$ and $D < 0$ for $\beta > \beta_*$ near the local bifurcation boundary $\gamma = \gamma_0$.

When $\mu > 1$, we have $\gamma_2 < 0$ and the determinant is always negative near the local bifurcation boundary $\gamma = \gamma_0$. When $\mu = 1$, we have $\beta = \gamma$ and $P = Q$, such that $D = 0$.

With the standard linearization, the stability problem for vector solitons reduces to the matrix eigenvalue problem $\hat{L}_+ \mathbf{u} = -\lambda \mathbf{w}$ and $\hat{L}_- \mathbf{w} = \lambda \mathbf{u}$, where $\mathbf{u}$ is a two-vector of real parts of the perturbation and $\mathbf{w}$ is a two-vector of imaginary parts of the perturbation, for a real eigenvalue λ. The matrix Schrodinger operators are

$$\hat{L}_+ = \begin{pmatrix} \beta - \Delta - V(\delta + 3\Phi^2 + \mu\Psi^2) & -2\mu V \Phi\Psi \\ -2\mu V \Phi\Psi & \gamma - \Delta - V(\delta + 3\Psi^2 + \mu\Phi^2) \end{pmatrix}$$

$$\hat{L}_- = \begin{pmatrix} \beta - \Delta - V(\delta + \Phi^2 + \mu\Psi^2) & 0 \\ 0 & \gamma - \Delta - V(\delta + \Psi^2 + \mu\Phi^2) \end{pmatrix}$$

Because $\hat{L}_-$ is a diagonal composition of two scalar Schrödinger operators, each has a simple zero eigenvalue with the ground state Φ and Ψ; therefore, the operator $\hat{L}_-$ is non-negative. Therefore, stability of fundamental vector solitons is determined by the number of negative eigenvalues of the matrix operator $\hat{L}_+$, similar to [13].

We compute the number of negative eigenvalues of the operator $\hat{L}_+$ near the local bifurcation point. When $\gamma = \gamma_0$ and $\Psi = 0$, we have

$$\hat{L}_+ = \begin{pmatrix} L_+ & 0 \\ 0 & L_0 \end{pmatrix} \tag{15}$$

such that the operator L_+ has exactly one negative eigenvalue (by the assumption that the scalar soliton is stable for $\beta > \beta_0$) and the operator L_0 has a simple zero eigenvalue with the eigenfunction ψ. We study bifurcation of the simple zero eigenvalue of L_0 for $\gamma \neq \gamma_0$. Using the same small parameter ϵ as in the local bifurcation analysis, we are looking for solution of the eigenvalue problem $\hat{L}_+ \mathbf{u} = \lambda \mathbf{u}$ by the regular perturbation theory $u_1 = \epsilon U_1 + O(\epsilon^3)$, $u_2 = \psi + \epsilon^2 U_2 + O(\epsilon^4)$, and $\lambda = \epsilon^2 \lambda_2 + O(\epsilon^4)$.

By algorithmic computations of the regular perturbation theory, we have the linear inhomogeneous problem for the first-order correction, $L_+ U_1 = 2\mu V(x, y)\phi\psi^2$, which is solvable with the solution $U_1 = 2\Phi_2$. Furthermore,

we have the linear inhomogeneous problem for U_2,

$$L_0 U_2 = (\lambda_2 - \gamma_2)\psi + 2\mu V(x, y)\phi\psi\,\Phi_2 + 3V(x, y)\psi^3 + 2\mu V(x, y)\phi\psi\,U_1,$$

with the solvability condition

$$\lambda_2 = \gamma_2 - \frac{6\mu(\psi^2, V(x, y)\phi\Phi_2) + 3(\psi^2, V(x, y)\psi^2)}{(\psi, \psi)} = -2\gamma_2.$$

When $\mu < 1$, we have $\gamma_2 > 0$, such that the zero eigenvalue of L_0 becomes a negative eigenvalue of $\hat{L}_+$. As a result, we have two negative eigenvalues of $\hat{L}_+$ near the local bifurcation boundary. Because $p'(\beta) > 0$, we have two positive eigenvalues of the Hessian matrix when $D > 0$ and one positive eigenvalue when $D < 0$. In the former case, the vector soliton is stable, while it is unstable in the latter case. Therefore, the boundary of $D = 0$ separates the domains of stability and instability of vector solitons on the plane (β, γ) in the assumption that the number of negative eigenvalues of $\hat{L}_+$ remains unchanged in the entire existence domain.

When $\mu > 1$, we have $\gamma_2 < 0$, such that the zero eigenvalue of L_0 becomes a positive eigenvalue of $\hat{L}_+$. As a result, we have only one negative eigenvalue of $\hat{L}_+$ near the local bifurcation boundary. In the same region, we have exactly one positive eigenvalue of the Hessian matrix, because $D < 0$. Therefore, the vector soliton is stable near the local bifurcation boundary. Numerics show that there exists a curve $D = 0$ in the existence domain (see Figure 4(b)), where the positive eigenvalue of the Hessian matrix crosses zero and becomes negative eigenvalue. These curves approach the bifurcation curves asymptotically for large (β, γ), because $D < 0$ on the bifurcation curves. In the assumption that the number of negative eigenvalues of $\hat{L}_+$ remains unchanged in the entire existence domain, the curve $D = 0$ separates the stability and instability domains.

When $\mu = 1$, we have $\gamma = \beta$ and the zero eigenvalue of L_0 is preserved as the zero eigenvalue of $\hat{L}_+$ in the entire existence domain $\beta = \gamma > \beta_0$. This additional eigenvalue is related to an arbitrary polarization of the vector soliton in the case $\mu = 1$: $\Phi = \cos\theta\phi$ and $\Psi = \sin\theta\phi$, where ϕ solves the scalar problem (6). The operator $\hat{L}_+$ always has a single negative eigenvalue (because we have verified numerically that L_+ has a single negative eigenvalue for $\beta > \beta_0$). Therefore, the vector soliton must be linearly stable in the case $\mu = 1$ for any $\beta > \beta_0$ (excluding the limit $\beta \to \infty$).

6. Conclusions

We have demonstrated that stable two-dimensional vector solitons can be supported by a nonlinear PCF structure with the Kerr nonlinearity. They constitute a class of two-component spatially localized modes that bifurcate from

their one-component scalar counterparts and are described by two independent parameters. Both scalar and vector solitons provide a generalization of the guided mode trapped in the PCF core to the nonlinear case, being confined by both linear and self-induced nonlinear refractive indices. The periodic PCF environment also provides an effective stabilization mechanism for these localized modes, in a sharp contrast with an entirely homogeneous nonlinear Kerr medium where both scalar and vector spatial solitons are unstable and may undergo the collapse instability. We have applied the analytical matrix criterion for stability of these PCF vector solitons, and have verified that this criterion is confirmed by the direct simulations of the soliton dynamics.

Acknowledgments

References

1. P. RUSSELL, Photonic crystal fibers, *Science* 299:358 (2003).
2. J. C. KNIGHT, Photonic crystal fibers, *Nature* 424:847 (2003).
3. Y. S. KIVSHAR and G. P. AGRAWAL, *Optical Solitons: From Fibers to Photonic Crystals*, Academic, San Diego, 2003.
4. Y. V. KARTASHOV, A. S. ZELENINA, V. A. VYSLOUKH, and L. TORNER, Stabilization of vector solitons in optical lattices, *Phys. Rev. E* 70:066623 (2004).
5. Z. CHEN, A. BEZRYADINA, I. MAKASYUK, and J. YANG, Observation of two-dimensional lattice vector solitons, *Opt. Lett.* 29:1656 (2004).
6. S. F. MINGALEEV and Y. S. KIVSHAR, Self-trapping and stable localized modes in nonlinear photonic crystals, *Phys. Rev. Lett.* 86:5474 (2001).
7. A. FERRANDO, M. ZACARÉS, P. FERNANDEZ DE CÓRDOBA, D. BINOSI, and J. A. MONSORIU, Spatial soliton formation in photonic crystal fibers, *Opt. Exp.* 11:452 (2003).
8. A. FERRANDO, M. ZACARÉS, P. FERNANDEZ DE CÓRDOBA, D. BINOSI, and J. A. MONSORIU, Vortex solitons in photonic crystal fibers, *Opt. Exp.* 12:817 (2004).
9. J. N. MALMBERG, A. H. CARLSSON, D. ANDERSON, M. LISAK, E. A. OSTROVSKAYA, and Y. S. KIVSHAR, Vector solitons in $(2 + 1)$ dimensions, *Opt. Lett.* 25:643 (2000).
10. J. E. DENNIS and R. B. SCHNABEL, *Numerical Methods for Unconstrained Optimization and Nonlinear Equations*, Prentice-Hall, Englewood Cliffs, NJ, 1983.
11. W. H. PRESS, S. A. TEUKOLSKY, W. T. VETTERLING, and B. P. FLANNERY, *Numerical Recipes in C*, 2nd ed. Cambridge University Press, Cambridge, 1992.
12. C. C. PAIGE and M. A. SAUNDERS, Solution of sparse indefinite systems of linear equations, *SIAM J. Numer. Anal.* 12:617 (1975).

13. D. E. PELINOVSKY and Y. S. KIVSHAR, Stability criterion for multicomponent solitary waves, *Phys. Rev. E* 62:8668 (2000).

14. D. E. PELINOVSKY, Intertia law for spectral stability of solitary waves in coupled nonlinear Schroedinger equations, *Proc. Roy. Soc. Lond. A* 461:783 (2005).

15. D. E. PELINOVSKY and J. YANG, Internal oscillations and radiation damping vector solitons, *Stud. Appl. Math.* 105:245 (2000).

16. J. YANG and D. E. PELINOVSKY, Stable vortex and dipole vector solitons in a saturable nonlinear medium, *Phys. Rev. E* 67:016608 (2003).

17. D. E. PELINOVSKY and J. YANG, Instabilities of multi-hump vector solitons in coupled nonlinear schrodinger equations, *Stud. Appl. Math.* 115:521 (2005).

THE AUSTRALIAN NATIONAL UNIVERSITY
MCMASTER UNIVERSITY
UNIVERSIDAD DE VIGO, SPAIN